Scanning transmission electron microscope analysis of amorphous-Si insertion layers prepared by catalytic chemical vapor deposition, causing low surface recombination velocities on crystalline silicon wafers

Koichi Higashimine and Koichi Koyama
Japan Advanced Institute of Science and Technology and JST-CREST, 1-1 Asahidai, Nomishi, Ishikawa 923-1292, Japan

Keisuke Ohdaira
Japan Advanced Institute of Science and Technology, 1-1 Asahidai, Nomishi, Ishikawa 923-1292, Japan

Hideki Matsumura and N. Otsuka[a)]
Japan Advanced Institute of Science and Technology and JST-CREST, 1-1 Asahidai, Nomishi, Ishikawa 923-1292, Japan

(Received 11 January 2012; accepted 6 April 2012; published 26 April 2012)

Microstructures of stacked silicon-nitride/amorphous-silicon/crystalline-silicon (SiN_x/*a*-Si/*c*-Si) layers prepared by catalytic chemical vapor deposition were investigated with scanning transmission electron microscopy to clarify the origin of the sensitive dependence of surface recombination velocities (SRVs) of the stacked structure on the thickness of the *a*-Si layer. Stacked structures with *a*-Si layers with thicknesses greater than 10 nm exhibit long effective carrier lifetimes, while those with thin *a*-Si layers have very short effective carrier lifetimes. A remarkably close correlation was found between the dependence of interface structures on the thicknesses of *a*-Si layers and the SRVs. In samples with *a*-Si layers less than 10 nm thick, significant damage occurred in *c*-Si wafers close to the interfaces, while those near *a*-Si layers larger than 10 nm remained nearly defect-free during observations over long periods. The observation of stacked structures without an SiN_x layer, along with energy dispersive spectroscopy and secondary ion mass spectroscopy analyses of nitrogen atom distributions, suggest that the preferential damage in *c*-Si wafers with thin *a*-Si layers is caused by nitrogen atoms in the interface regions of *c*-Si wafers that diffuse during the growth of SiN_x layers. © *2012 American Vacuum Society*.
[http://dx.doi.org/10.1116/1.4706894]

I. INTRODUCTION

High-quality surface passivation is required for crystalline silicon (*c*-Si) solar cells to achieve high conversion efficiency. In particular, sufficient surface passivation is essential for high-efficiency back-contact solar cells in which photogenerated carriers must diffuse over long distances in lateral directions. In a recent study, Koyama *et al.* showed that remarkably low surface recombination velocities (SRVs) were obtained with silicon-nitride/amorphous-silicon (SiN_x/*a*-Si) stacked layers formed by catalytic chemical vapor deposition (Cat-CVD), which is also referred to as hot-wire CVD.[1] SRVs lower than 1.5 cm/s and 9.0 cm/s were obtained for *n*-type and *p*-type *c*-Si wafers, respectively. The significance of these results is that the temperature throughout the formation of the stacked layers was lower than 250 °C. It is well known that SRVs of excess carriers can be decreased to the order of 1 cm/s when *c*-Si surfaces are passivated by thermally grown silicon-dioxide (SiO_2) films. For example, a stacked structure consisting of a thermally grown SiO_2 film and plasma-enhanced chemical-vapor-deposited SiN_x showed excellent passivation ability with SRVs below 2.4 cm/s with an *n*-type Si wafer.[2] Such excellent passivation with an SiO_2 film, however, requires processing at temperatures higher than 900 °C. Low-temperature passivation techniques are generally preferred to prevent the degradation of Si bulk quality and to decrease processing times. In particular, high-temperature processes are likely to result in serious problems when thin large wafers are used in *c*-Si solar cells.

In the present study we observed SiN_x/*a*-Si/*c*-Si stacked structures prepared by Cat-CVD with scanning transmission electron microscopy (STEM). In the above-mentioned study, Koyama *et al.* found that the SRV of the stacked structure depends sensitively on the thickness of an *a*-Si insertion layer.[1] With *a*-Si layer thicknesses below 10 nm or in the absence of an *a*-Si layer, the effective carrier lifetime (τ_{eff}) is significantly shorter than in structures with thicker *a*-Si layers. The present observations, therefore, were focused on the change in structure of *c*-Si crystals at the interface with decreasing *a*-Si layer thickness. In earlier studies on electronic structures of semiconductor interfaces such as those of SiO_2/Si interfaces, a variety of complementary experimental techniques have been employed, including spectroscopic and microscopic techniques, for investigating electronic structures relevant to surface recombination of excess carriers.[3] One cannot, therefore, expect that an STEM observation alone is able to clarify the structural origin responsible for surface carrier recombination in this system. In the present study, however, we found a remarkably close correlation between the dependence of interface structures revealed by STEM images

[a)]Electronic mail: ootsuka@jaist.ac.jp

on the thicknesses of *a*-Si layers and that of SRVs. Structures of *c*-Si wafers with thin *a*-Si layers or without an *a*-Si layer degraded rapidly at the interface during the observation, while those with thick *a*-Si layers retained nearly perfect structures throughout the observation. The observation of stacked structures without an SiN_x layer, along with energy dispersive spectroscopy (EDS) and secondary ion mass spectroscopy (SIMS) analyses of nitrogen distributions, suggest that the preferential damage formation in *c*-Si wafers with thin *a*-Si layers is caused by N atoms in the interfacial region of *c*-Si that diffused during the growth of SiN_x layers. These results provide us with an important insight into the structural origin of surface carrier recombination in this system.

II. EXPERIMENT

SiN_x/*a*-Si/*c*-Si stacked structures with different *a*-Si layer thicknesses and one sample without an *a*-Si layer were prepared by Cat-CVD. Table I lists the six samples for which structures and effective carrier lifetimes were investigated in this study. The procedure for the preparation of SiN_x/*a*-Si/*c*-Si stacked structures was described in detail in an earlier report.[1] Phosphorus-doped *n*-type (100) floating-zone-Si wafers with resistivity 2.5 Ω cm, thickness 290 μm, and mirror-polished surfaces on both sides were used. After cleaning with 5% diluted hydrofluoric acid, wafers were transferred to the load-lock chamber of a Cat-CVD system. Two chambers were used for intrinsic *a*-Si and SiN_x deposition, with wafers transferred from one chamber to the other via the load-lock chamber. For the deposition of *a*-Si layers, the gas pressure was 0.55 Pa, the substrate–catalyzer distance was 12 cm, the silane flow rate was 10 cubic centimeter per minute at STP (SCCM), and the temperature of the tungsten wire used as catalyzer was 1800 °C. The deposition rate of *a*-Si layers was 30 nm/min and substrate temperatures were set at 150 °C for samples T2, T5, T10, and T30. For sample T10′, the *a*-Si layer was grown at 90 °C. The thickness of SiN_x layers was fixed at 100 nm for all samples. For the deposition of SiN_x layers, the gas pressure was 10 Pa, the substrate–catalyzer distance was 8 cm, the substrate temperature was 250 °C, and the temperature of the tungsten wire used as a catalyzer was 1800 °C. The flow rates of silane and ammonia gases were 8.5 and 200 SCCM, respectively. The deposition rate of SiN_x layers was 34 nm/min. The τ_{eff} values of the passivated Si wafers were measured at room temperature by a microwave-detection photoconductivity decay method with a Kobelco LTA-1510EP instrument. The excess carriers were generated by a laser pulse at wavelength 904 nm and photon density 5×10^{13} cm^{-2}.

TABLE I. Effective carrier lifetimes, τ_{eff}, and layer thicknesses of the six samples.

Sample	SiN_x layer (nm)	*a*-Si layer (nm)	Substrate temperature for *a*-Si (°C)	τ_{eff} (μs)
T30	100	30	150	7320
T10	100	10	150	9710
T5	100	5	150	3340
T2	100	2	150	610
T0	100	—	150	210
T10'	100	10	90	10 760

For STEM observations, {110}cross-sectional samples were prepared by the focused ion beam method, with Ga ions at kinetic energies of 30 keV for rough thinning and at 5 and 2 keV for fine thinning. The final polishing was carried out by using a gentle milling system with Ar ions at kinetic energies of 1 keV and 200 eV to remove the amorphous layers formed by irradiation of the Ga beam. Each sample was cleaned for 10 min using an ion cleaner with an electric glow discharge at 300 V to remove contamination of hydrocarbons immediately before the STEM observation. For observations, a JEM-ARM200F STEM from JEOL with spherical aberration correction with a condenser lens system was used. An EDS system was attached to the microscope for the analysis of element distributions. A condenser aperture and a bright field aperture with diameters of 30 μm and 3 mm, respectively, were used. The acceptance angles for detection of scattered electrons ranged from 67 to 250 mrad for high angle annular dark field (HAADF) images.

III. RESULTS

A. STEM analysis of the effect of the thicknesses of a-Si layers on damage formation

The effective carrier lifetimes of the six samples are listed in Table I. Further results for τ_{eff} were presented in an earlier report.[1] From these results, one can see strong dependence of τ_{eff} on the thickness of the *a*-Si layer. The τ_{eff} was 210 μs for sample T0, whose *c*-Si wafer was passivated only by an SiN_x layer, and increased with the insertion of an *a*-Si layer. It also increased with increasing *a*-Si layer thickness up to 10 nm and remained nearly constant for samples T10 and T30. As presented in the earlier report,[1] a similar tendency was observed for *p*-type Si wafers.

Figures 1(a)–1(d) are HAADF images of samples T30, T10, T5, and T0, respectively. These images were recorded after the observation of the same areas for approximately 3 min with a probe current of 7 pA at 200 kV. HAADF images of samples T30 and T10 show nearly perfect crystalline structures of *c*-Si wafers from their interior to the interfaces with *a*-Si layers. These images also show that the interfaces are remarkably flat on the atomic scale, as seen in a magnified image of the interface of sample T10 in Fig. 1(e). The images of samples T30 and T10 did not change over long periods of observation extending over 15 min. HAADF images of the other two samples T5 and T0, on the other hand, show highly defective structures of the *c*-Si wafers in the neighborhood of their interfaces with either a thin *a*-Si or SiN_x layer, as seen in Figs. 1(c) and 1(d). Broad dark contrasts are spread over the interface regions of *c*-Si wafers where images of Si atom columns are almost invisible. The dark contrasts may be caused by extended defects resulting from aggregation of vacancies and interstitial Si atoms or amorphous structures. These defect structures were found to develop during the observation; images of *c*-Si wafers of samples T5 and T0 were similar to those of Figs. 1(a) and 1(b) at the beginning of the observation. A similar tendency was observed in sample T2.

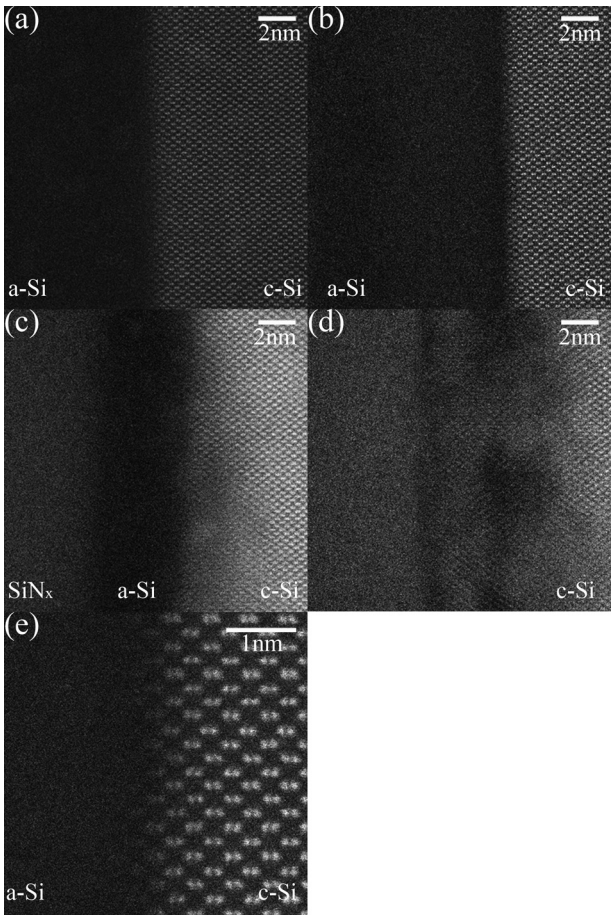

FIG. 1. HAADF images of samples (a) T30, (b) T10, (c) T5, (d) T0, and (e) magnified HAADF image of the interface of sample T10.

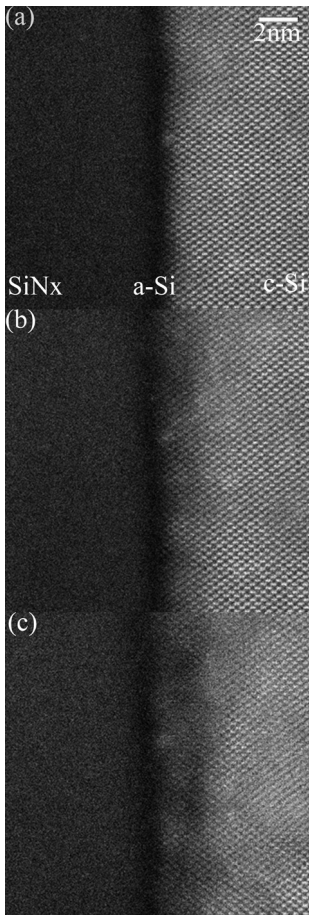

FIG. 2. Series of three HAADF images taken from the same area of sample T2.

Because two groups appear to be divided between samples T5 and T10, we made repeated observations of these two samples. For samples T5 and T10, we prepared two and three cross-sectional samples, respectively, and made observations of several different interface areas for each cross-sectional sample. We obtained the same results for all observations as those shown in Figs. 1(b) and 1(c) for samples T10 and T5, respectively. This implies that there is a distinctive difference between these two samples in their susceptibilities to radiation damage, although the thicknesses of their *a*-Si layers differed from each other by only 5 nm.

We next made observations of the process of defect structure formation in samples with thin *a*-Si layers. For this observation we used an accelerating voltage of 120 kV, which was expected to slow the rate of defect formation caused by electron irradiation. Figure 2 shows a series of three HAADF images taken from the same area of sample T2. The image in Fig. 2(a) was recorded at the beginning of the observation, and those of Figs. 2(b) and 2(c) were recorded successively with time intervals of 90s. These images show that defects were formed initially at the interface and spread over the interior of the *c*-Si wafer. In Fig. 2(a), one can see small areas of dark contrast near the interface, while the rest of the *c*-Si wafer exhibits an image of a nearly perfect crystalline structure. Similar defect formation processes were observed in samples T5 and T0.

The above-presented observation of HAADF images shows that damage occurred preferentially in interfacial regions of *c*-Si wafers in samples T5, T2, and T0 by electron irradiation, as demonstrated in Fig. 2(a) for sample T2. At the beginning of the observation, on the other hand, the interfacial areas of *c*-Si wafers of all five samples appear to be similar to one another in the HAADF images. To find a difference in the original interface structure between the two groups of samples, we made detailed analyses of HAADF images and EDS profiles of element distributions for five samples during the early stage of the observations. From EDS analysis, we found an important difference in the N atom distribution between two groups of samples. Figures 3(a) and 3(b) are Si and N atom distributions in samples T2 and T10, respectively, obtained by EDS measurement. The location of the *a*-Si layer corresponds to a region between the two vertical lines in each figure. The EDS profiles show that the density of N atoms gradually decreases from the SiN_x/*a*-Si interface toward the *c*-Si wafer. In sample T2, an appreciable number of N atoms diffused into the *c*-Si wafer through the *a*-Si layer, while diffused N atoms appear to be confined inside the *a*-Si layer of sample T10. These results indicate that a thick *a*-Si layer effectively prevents diffusion of N atoms into a *c*-Si wafer, which occurs during the growth of an SiN_x layer.

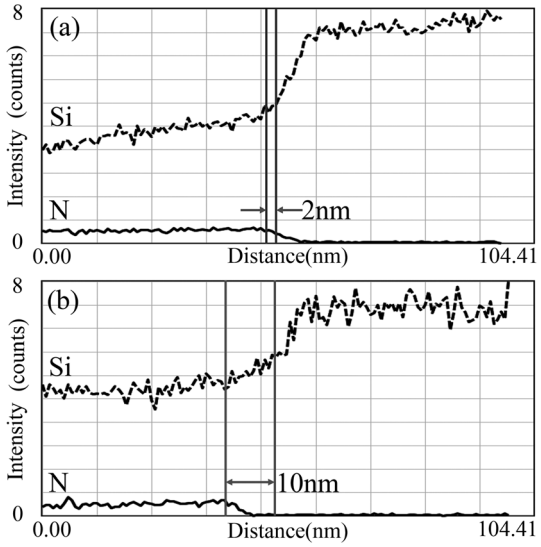

FIG. 3. EDS profiles of Si and N atom distributions in samples (a) T2 and (b) T10.

Because of the above-mentioned results, we closely examined the intensity profiles of HAADF images for samples T10 and T2. Figures 4(a) and 4(b) show intensity profiles of samples T10 and T2, respectively, with corresponding HAADF images of their interfaces. In Fig. 4(a), one can see that the amplitude of the intensity oscillation due to the periodic arrangement of Si atom rows is nearly constant over the whole observed area of the *c*-Si of sample T10, although there are certain fluctuations in the intensity amplitude. In the case of sample T2, on the other hand, the amplitude of the intensity oscillation gradually decreases toward the *a*-Si/*c*-Si interface. The origin of this oscillation damping is not currently clear. It may, however, be attributed to the existence of N-related defect complexes in the interface region of *c*-Si, as discussed later, because sample T2 had a considerable quantity of N atoms in that region, as shown in Fig. 3(a).

B. STEM analysis of the effect of the growth temperature on damage formation

Figure 5(a) shows an HAADF image of sample T10′. Similar to sample T10, which has an *a*-Si layer with the same thickness (10 nm), no significant damage formed in *c*-Si during observation over a long period of time. The *a*-Si layer in sample T10′ was grown at 90 °C, which was lower than that of sample T10. It was reported that the hydrogen concentration increases at a lower growth temperature.[4] The result for sample T10′, however, does not show a significant effect of an increase in the hydrogen concentration on the diffusion of N atoms. If there was such an effect, damage would develop during the STEM observation, as in the cases of samples T5, T2, and T0. Corresponding to this result, the τ_{eff} of sample T10′ is comparable to that of sample T10. To examine the effect of low growth temperature, we also observed a sample whose SiN_x layer was grown at room temperature. The *a*-Si layer in this sample was grown at 90 °C to a thickness of 10 nm. As shown in Fig. 5(b), no significant damage was found in the *c*-Si during the observation of this sample.

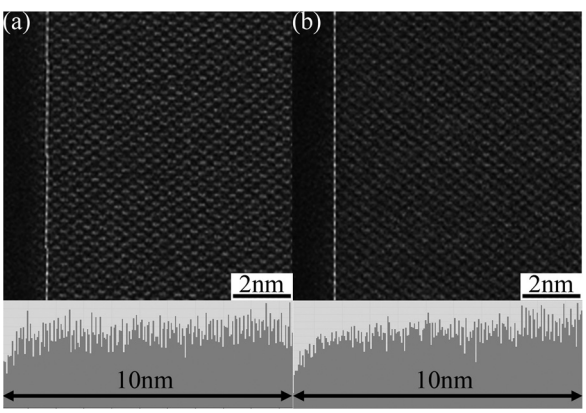

FIG. 4. HAADF images of samples (a) T10 and (b) T2, with intensity profiles. The images were recorded immediately after the start of the observation.

C. SIMS analysis of nitrogen atom distribution

To examine the distribution of N atoms in *c*-Si wafers more quantitatively, we made SIMS analyses of two samples, SIMS-1 and SIMS-2. Sample SIMS-1 was a *c*-Si wafer and sample SIMS-2 was a *c*-Si wafer with a 10-nm-thick *a*-Si cap layer. The surfaces of the *c*-Si wafers were prepared by the same method as that of the five samples T30–T0. The 10-nm-thick *a*-Si cap layer was deposited at gas pressure 1 Pa, silane flow rate 10 SCCM, catalyzer temperature 1800 °C, and substrate temperature 90 °C. Two samples were exposed to NH_3 at 250 °C for 10 s with a gas pressure of 10 Pa, flow rate 200 SCCM, and catalyzer temperature 1800 °C, which were similar conditions to that of the deposition of SiN_x layers for the above-mentioned five samples. SIMS measurements were carried out with Cs^+ ions at an acceleration voltage of 1.0 kV. Figures 6(a) and 6(b) are N atom density profiles obtained by SIMS measurements for samples SIMS-1 and SIMS-2, respectively, with their schematic sample structures shown in the insets. According to the SIMS measurement, the hydrogen concentration was nearly constant at approximately $1.0 \times 10^{21}\,cm^{-3}$ over the *a*-Si layer in sample SIMS-2. Two profiles show that the N atom density decreased from the surface in an identical manner for both samples, implying that N atoms diffuse at similar rates in the *c*-Si wafer and *a*-Si layer. In sample SIMS-2, the N atom density was $1 \times 10^{20}\,cm^{-3}$ at 5 nm below the

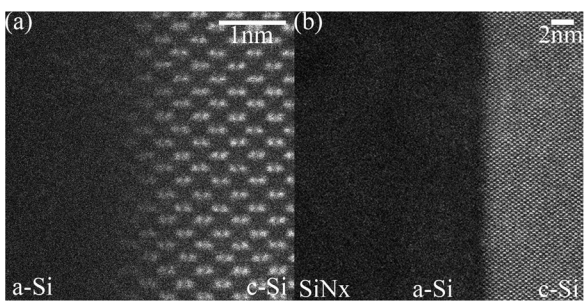

FIG. 5. HAADF images of (a) sample T10′ and (b) an SiN_x/*a*-Si/*c*-Si stacked structure with an SiN_x layer grown at room temperature.

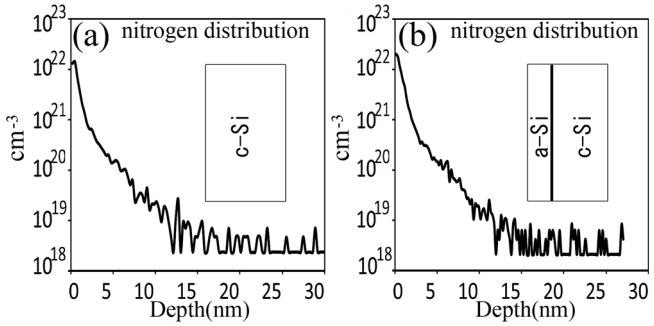

FIG. 6. SIMS profiles of N atom distributions in samples (a) SIMS-1 and (b) SIMS-2.

surface, while it was $1 \times 10^{19}\,\mathrm{cm}^{-3}$ at a 10 nm depth. This indicates that the N atom densities at *a*-Si/*c*-Si interfaces of sample T10 were significantly lower than those of sample T5. The most probable impurities diffusing into the *c*-Si wafer during the deposition of SiN_x are hydrogen and N atoms. H atoms were also supplied during deposition of *a*-Si, but N atoms were supplied only for deposition of SiN_x. Defects were created only when significant amounts of N atoms were present at the interface of *c*-Si, as shown in Figs. 3 and 6. From these results, one can suggest that damage formation by electron irradiation in sample T5 and the other two samples, T2 and T0, is assisted by the N atoms that diffused into *c*-Si wafers during the deposition of the SiN_x layers. One can also explain the significantly different susceptibility to damage formation between samples T10 and T5 as resulting from the large difference in N atom densities at the *a*-Si/*c*-Si interfaces of these two samples.

D. STEM analysis of a-Si/c-Si stacked structures

To verify the above-presented possibility further, we made STEM observations of *c*-Si wafers with only thin *a*-Si cap layers in the thickness range from 2.7 to 18 nm. Figures 7(a) and 7(b) are HAADF images of a *c*-Si wafer with a 2.7-nm-thick *a*-Si cap layer. The cap layer was deposited under the same conditions as those of sample SIMS-2. The former image was taken immediately after the start of the observation, and the latter was recorded after observation for 15 min. As shown in these images, no significant damage occurred during the observation. This result clearly differs from those for samples T2 and T5, which also have similarly thin *a*-Si layers but are covered by SiN_x layers. The same result was obtained for other samples with thicker *a*-Si cap layers.

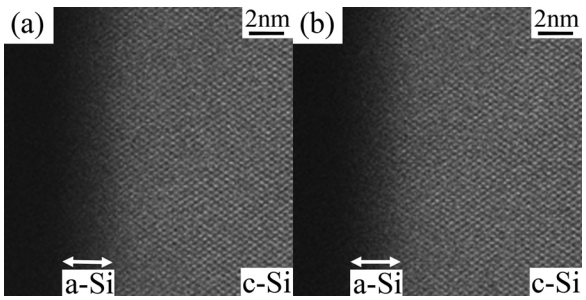

FIG. 7. HAADF images of a *c*-Si wafer with a 2.7-nm-thick *a*-Si layer. Image (a) was recorded immediately after the start of the observation and image (b) was recorded after observation for 15 min. The left side of the *a*-Si layer in each image is a carbon film, coated during the preparation of the cross-sectional sample.

IV. DISCUSSION

It was reported that the deposition of a SiN_x film on an Si wafer at a low temperature induces a stress in the Si wafer.[5] One may therefore consider the possibility that defect formation by electron irradiation is assisted by the stress induced by the SiN_x film. In the present experiments, both front and back sides of an Si wafer were symmetrically covered by identical films for all SiN_x/*a*-Si/*c*-Si stacked structures.[1] Hence, the stress due to the deposited SiN_x films uniformly extended over the entire Si wafer. It is therefore unlikely that such a uniformly distributed stress assisted defect formation only in the interfacial region. It is also difficult to explain the significantly different susceptibilities to damage formation between samples T10 and T5 on the basis of the stress induced by an SiN_x film. From these observations, we conclude that damage formation in *c*-Si wafers is assisted by N atoms that diffuse during the growth of an SiN_x layer.

Before now, extensive studies were carried out on damage formation by electron irradiation in *a*-Si.[6,7] These studies showed that H atoms in *a*-Si migrate from electron-irradiated regions and contribute to damage formation. In contrast, the present results indicate that such an H-related process does not play a major role in the damage formation in SiN_x/*a*-Si/*c*-Si stacked structures. There is also the possibility that the presence of a high concentration of hydrogen may assist N atom diffusion through an *a*-Si layer. As shown in Sec. III C, no indication of such an effect has been found. In the present study, however, we examined samples grown under a limited range of conditions. It is therefore necessary to carry out further systematic study to clarify this possibility, because high concentration of hydrogen in *a*-Si layers and Si crystals are believed to have significant effects on atomic and electronic processes.

The results presented in this paper strongly suggest that N atoms that have diffused into a *c*-Si wafer promote damage formation during STEM observations. This possibility is further supported by the results of an earlier TEM study on N-doped Si crystals, which showed that the presence of N atoms significantly enhanced damage formation by electron irradiation.[8] Frenkel pair defect generation and interaction with N impurities under a 200 kV TEM beam were observed in Czochralski Si doped with N atoms of $10^{15}\,\mathrm{cm}^{-3}$, while there was no effect in nitrogen-free silicon. It was suggested that during irradiation, the Frenkel pairs of vacancies and interstitial atoms that were created by electron irradiation did not recombine because of the presence of N atoms. Nitrogen atoms are believed to form complexes with newly formed vacancies, permanently separating the interstitial silicon of the Frenkel pair from its vacancy and resulting in the formation of extended defects. If significant diffusion of nitrogen

atoms into interfacial regions of *c*-Si wafers occurs during the deposition of SiN_x layers on samples with a thin *a*-Si layer or in the absence of an *a*-Si layer, preferential defect formation is expected to occur through this process.

As explained earlier, we found a remarkably close correlation of the results of the STEM observation with those of SRV measurements for SiN_x/*a*-Si/*c*-Si stacked structures. In the case of samples with *a*-Si layers with thicknesses below 10 nm, significant damage formation occurs in *c*-Si wafers close to the interface, whereas the τ_{eff} of such samples were found to be significantly shorter than those with *a*-Si layers of thickness greater than 10 nm. The results of the STEM observations and SIMS measurements strongly suggest that the preferential formation of radiation damage in samples T5, T2, and T0 was assisted by N atoms that diffused into the interfacial regions of the *c*-Si wafers. There is, therefore, the possibility that the short τ_{eff} durations of samples T5, T2, and T0 were also caused by N atoms in their interfacial regions. A number of earlier studies on N-doped Si showed that N atoms form defect complexes comprising N atom pairs and vacancies.[9–11] These defect complexes are believed to form deep levels and act as carrier traps.[12,13] The results of the present study, hence, suggest that N-related defect complexes may play a major role in surface recombination of photoexcited carriers in *c*-Si wafers passivated by SiN_x layers.

As reported in the earlier report,[1] on the other hand, an SiN_x layer makes a significant contribution to long carrier lifetimes in samples with relatively thick *a*-Si layers. For an *a*-Si layer with the 10 nm thickness, the *a*-Si/*c*-Si stacked structures without an SiN_x layer have significantly short carrier lifetimes compared with those of the SiN_x/*a*-Si/*c*-Si stacked structures. The short carrier lifetimes of *a*-Si/*c*-Si stacked structures are attributed to trapping of carriers at the surface of the *a*-Si layer. The SiN_x layer is believed to passivate this surface and drive carriers back toward *c*-Si with its high potential barriers for both electrons and holes. If an *a*-Si layer is too thick, the latter effect is apparently weakened, as seen in the reduction of τ_{eff} for T30 compared with that of T10. On the basis of the current results and those of the earlier study,[1] there should be an optimum thickness for the *a*-Si layer for the SiN_x/*a*-Si/*c*-Si stacked structure with respect to carrier lifetime. Because N atom diffusion is involved in the problem, such an optimum thickness is believed to depend on the growth condition of the stacked structure. For the growth conditions of the samples examined in the present study, 10 nm appears to be the optimum thickness.

V. SUMMARY AND CONCLUSION

SiN_x/*a*-Si/*c*-Si stacked structures prepared by Cat-CVD were investigated with STEM to clarify the origin of the sensitive dependence of SRVs of the stacked structure on the thickness of the *a*-Si layer. A remarkably close correlation between the dependence of interface structures revealed by STEM images on the thicknesses of *a*-Si layers and that of SRVs was found in the study. In the case of samples with *a*-Si layers with thicknesses below 10 nm, preferential damage occurs in *c*-Si wafers close to the interface, while *c*-Si wafers with *a*-Si layers of thickness greater than 10 nm remain nearly defect-free during observations over long periods of time. From the observation of stacked structures without an SiN_x layer, along with EDS and SIMS analyses of nitrogen distributions, it is concluded that the preferential damage formation in *c*-Si wafers with thin *a*-Si layers is caused by nitrogen atoms in the interface regions of *c*-Si wafers diffusing during the growth of SiN_x layers.

[1] K. Koyama, K. Ohdaira, and H. Matsumura, Appl. Phys. Lett. **97**, 082108 (2010).
[2] Y. Larionova, V. Mertens, N. Harder, and R. Brendel, Appl. Phys. Lett. **96**, 032105 (2010).
[3] F. J. Grunthaner and P. J. Grunthaner, Mater. Sci. Rep. **1**, 65 (1986).
[4] T. Unold, R. C. Reedy, and A. H. Mahan, J. Non-Cryst. Solids **227-230**, 362 (1998).
[5] M. Takano *et al.*, Jpn. J. Appl. Phys., Part 1 **44**, 4098 (2005).
[6] U. Schneider, B. Schroeder, and P. Lechner, J. Non-Cryst. Solids **115**, 63 (1989).
[7] A. Yelon, H. Fritzsche, and H. Branz, J. Non-Cryst. Solids 266-269, 437 (2000).
[8] N. Stoddard, A. Karoui, G. Duscher, A. Kvit, and G. Rozgonyi, Electrochem. Solid-State Lett. **6**, G134 (2003).
[9] H. J. Stein, Mater. Res. Soc. Symp. Proc. **59**, 523 (1986).
[10] R. Jones, S. Obrai, F. B. Rasmussen, and B. B. Nielsen, Phys. Rev. Lett. **72**, 1882 (1994).
[11] A. Karoui, F. S. Karoui, G. A. Rozgonyi, M. Hourai, and K. Sueoka, J. Electrochem. Soc. **150**, G771 (2003).
[12] Y. Tokumaru, H. Okushi, T. Masui, and T. Abe, Jpn. J. Appl. Phys., Part 2 **21**, L443 (1982).
[13] N. Fuma, K. Tashiro, K. Kakumoto, and Y. Takano, Jpn. J. Appl. Phys., Part 1 **35**, 1993 (1996).